



First evidence for the decay $B_s^0 \rightarrow \mu^+ \mu^-$

The LHCb collaboration

R. Aaij³⁸, C. Abellan Beteta^{33,n}, A. Adametz¹¹, B. Adeva³⁴, M. Adinolfi⁴³, C. Adrover⁶, A. Affolder⁴⁹, Z. Ajaltouni⁵, J. Albrecht³⁵, F. Alessio³⁵, M. Alexander⁴⁸, S. Ali³⁸, G. Alkhazov²⁷, P. Alvarez Cartelle³⁴, A.A. Alves Jr²², S. Amato², Y. Amhis³⁶, L. Anderlini^{17,f}, J. Anderson³⁷, R. Andreassen⁵⁷, R.B. Appleby⁵¹, O. Aquines Gutierrez¹⁰, F. Archilli^{18,35}, A. Artamonov³², M. Artuso⁵³, E. Aslanides⁶, G. Auremma^{22,m}, S. Bachmann¹¹, J.J. Back⁴⁵, C. Baesso⁵⁴, W. Baldini¹⁶, R.J. Barlow⁵¹, C. Barschel³⁵, S. Barsuk⁷, W. Barter⁴⁴, A. Bates⁴⁸, Th. Bauer³⁸, A. Bay³⁶, J. Beddow⁴⁸, I. Bediaga¹, S. Belogurov²⁸, K. Belous³², I. Belyaev²⁸, E. Ben-Haim⁸, M. Benayoun⁸, G. Bencivenni¹⁸, S. Benson⁴⁷, J. Benton⁴³, A. Berezhnoy²⁹, R. Bernet³⁷, M.-O. Bettler⁴⁴, M. van Beuzekom³⁸, A. Bien¹¹, S. Bifani¹², T. Bird⁵¹, A. Bizzeti^{17,h}, P.M. Bjørnstad⁵¹, T. Blake³⁵, F. Blanc³⁶, C. Blanks⁵⁰, J. Blouw¹¹, S. Blusk⁵³, A. Bobrov³¹, V. Bocci²², A. Bondar³¹, N. Bondar²⁷, W. Bonivento¹⁵, S. Borghi^{51,48}, A. Borgia⁵³, T.J.V. Bowcock⁴⁹, E. Bowen³⁷, C. Bozzi¹⁶, T. Brambach⁹, J. van den Brand³⁹, J. Bressieux³⁶, D. Brett⁵¹, M. Britsch¹⁰, T. Britton⁵³, N.H. Brook⁴³, H. Brown⁴⁹, A. Büchler-Germann³⁷, I. Burducea²⁶, A. Bursche³⁷, J. Buytaert³⁵, S. Cadceddu¹⁵, O. Callot⁷, M. Calvi^{20,j}, M. Calvo Gomez^{33,n}, A. Camboni³³, P. Campana^{18,35}, A. Carbone^{14,c}, G. Carboni^{21,k}, R. Cardinale^{19,i}, A. Cardini¹⁵, H. Carranza-Mejia⁴⁷, L. Carson⁵⁰, K. Carvalho Akiba², G. Casse⁴⁹, M. Cattaneo³⁵, Ch. Cauet⁹, M. Charles⁵², Ph. Charpentier³⁵, P. Chen^{3,36}, N. Chiapolini³⁷, M. Chrzyszcz²³, K. Ciba³⁵, X. Cid Vidal³⁴, G. Ciezarek⁵⁰, P.E.L. Clarke⁴⁷, M. Clemencic³⁵, H.V. Cliff⁴⁴, J. Closier³⁵, C. Coca²⁶, V. Coco³⁸, J. Cogan⁶, E. Cogneras⁵, P. Collins³⁵, A. Comerma-Montells³³, A. Contu^{15,52}, A. Cook⁴³, M. Coombes⁴³, G. Corti³⁵, B. Couturier³⁵, G.A. Cowan³⁶, D. Craik⁴⁵, S. Cunliffe⁵⁰, R. Currie⁴⁷, C. D'Ambrosio³⁵, P. David⁸, P.N.Y. David³⁸, I. De Bonis⁴, K. De Bruyn³⁸, S. De Capua⁵¹, M. De Cian³⁷, J.M. De Miranda¹, L. De Paula², P. De Simone¹⁸, D. Decamp⁴, M. Deckenhoff⁹, H. Degaudenzi^{36,35}, L. Del Buono⁸, C. Deplano¹⁵, D. Derkach¹⁴, O. Deschamps⁵, F. Dettori³⁹, A. Di Canto¹¹, J. Dickens⁴⁴, H. Dijkstra³⁵, P. Diniz Batista¹, M. Dogaru²⁶, F. Domingo Bonal^{33,n}, S. Donleavy⁴⁹, F. Dordei¹¹, P. Dornan⁵⁰, A. Dosil Suárez³⁴, D. Dossett⁴⁵, A. Dovbnya⁴⁰, F. Dupertuis³⁶, R. Dzhelyadin³², A. Dziurda²³, A. Dzyuba²⁷, S. Easo^{46,35}, U. Egede⁵⁰, V. Egorychev²⁸, S. Eidelman³¹, D. van Eijk³⁸, S. Eisenhardt⁴⁷, R. Ekelhof⁹, L. Eklund⁴⁸, I. El Rifai⁵, Ch. Elsasser³⁷, D. Elsby⁴², A. Falabella^{14,e}, C. Färber¹¹, G. Fardell⁴⁷, C. Farinelli³⁸, S. Farry¹², V. Fave³⁶, V. Fernandez Albor³⁴, F. Ferreira Rodrigues¹, M. Ferro-Luzzi³⁵, S. Filippov³⁰, C. Fitzpatrick³⁵, M. Fontana¹⁰, F. Fontanelli^{19,i}, R. Forty³⁵, O. Francisco², M. Frank³⁵, C. Frei³⁵, M. Frosini^{17,f}, S. Furcas²⁰, A. Gallas Torreira³⁴, D. Galli^{14,c}, M. Gandelman², P. Gandini⁵², Y. Gao³, J. Garofoli⁵³, P. Garosi⁵¹, J. Garra Tico⁴⁴, L. Garrido³³, C. Gaspar³⁵, R. Gauld⁵², E. Gersabeck¹¹, M. Gersabeck⁵¹, T. Gershon^{45,35}, Ph. Ghez⁴, V. Gibson⁴⁴, V.V. Gligorov³⁵, C. Göbel⁵⁴, D. Golubkov²⁸, A. Golutvin^{50,28,35}, A. Gomes², H. Gordon⁵², M. Grabalosa Gándara³³, R. Graciani Diaz³³, L.A. Granado Cardoso³⁵, E. Graugés³³, G. Graziani¹⁷, A. Grecu²⁶, E. Greening⁵², S. Gregson⁴⁴, O. Grünberg⁵⁵, B. Gui⁵³, E. Gushchin³⁰, Yu. Guz³², T. Gys³⁵, C. Hadjivasiliou⁵³, G. Haefeli³⁶, C. Haen³⁵, S.C. Haines⁴⁴, S. Hall⁵⁰, T. Hampson⁴³, S. Hansmann-Menzemer¹¹, N. Harnew⁵², S.T. Harnew⁴³, J. Harrison⁵¹, P.F. Harrison⁴⁵, T. Hartmann⁵⁵, J. He⁷, V. Heijne³⁸, K. Hennessy⁴⁹, P. Henrad⁵, J.A. Hernandez Morata³⁴, E. van Herwijnen³⁵, E. Hicks⁴⁹, D. Hill⁵², M. Hoballah⁵, C. Hombach⁵¹, P. Hopchev⁴, W. Hulsbergen³⁸, P. Hunt⁵², T. Huse⁴⁹, N. Hussain⁵², D. Hutchcroft⁴⁹, D. Hynds⁴⁸, V. Iakovenko⁴¹, P. Ilten¹², J. Imong⁴³, R. Jacobsson³⁵, A. Jaeger¹¹, E. Jans³⁸, F. Jansen³⁸, P. Jaton³⁶, F. Jing³, M. John⁵², D. Johnson⁵², C.R. Jones⁴⁴, B. Jost³⁵, M. Kaballo⁹, S. Kandybei⁴⁰, M. Karacson³⁵, T.M. Karbach³⁵, I.R. Kenyon⁴², U. Kerzel³⁵, T. Ketel³⁹, A. Keune³⁶, B. Khanji²⁰, O. Kochebina⁷, V. Komarov^{36,29}, R.F. Koopman³⁹, P. Koppenburg³⁸, M. Korolev²⁹, A. Kozlinskiy³⁸, L. Kravchuk³⁰, K. Kreplin¹¹, M. Kreps⁴⁵, G. Krocker¹¹, P. Krokovny³¹, F. Kruse⁹, M. Kucharczyk^{20,23,j}, V. Kudryavtsev³¹, T. Kvaratskheliya^{28,35}, V.N. La Thi³⁶, D. Lacarrere³⁵, G. Lafferty⁵¹, A. Lai¹⁵, D. Lambert⁴⁷, R.W. Lambert³⁹, E. Lanciotti³⁵, G. Lanfranchi^{18,35}, C. Langenbruch³⁵, T. Latham⁴⁵, C. Lazzeroni⁴², R. Le Gac⁶, J. van Leerdam³⁸, J.-P. Lees⁴, R. Lefèvre⁵, A. Leflat^{29,35}, J. Lefrançois⁷, O. Leroy⁶, T. Lesiak²³, Y. Li³, L. Li Gioi⁵, M. Liles⁴⁹, R. Lindner³⁵,

C. Linn¹¹, B. Liu³, G. Liu³⁵, J. von Loeben²⁰, J.H. Lopes², E. Lopez Asamar³³, N. Lopez-March³⁶, H. Lu³, J. Luisier³⁶, H. Luo⁴⁷, A. Mac Raighne⁴⁸, F. Machefert⁷, I.V. Machikhiliyan^{4,28}, F. Maciuc²⁶, O. Maev^{27,35}, M. Maino²⁰, S. Malde⁵², G. Manca^{15,d}, G. Mancinelli⁶, N. Mangiafave⁴⁴, U. Marconi¹⁴, R. Märki³⁶, J. Marks¹¹, G. Martellotti²², A. Martens⁸, L. Martin⁵², A. Martín Sánchez⁷, M. Martinelli³⁸, D. Martinez Santos³⁴, D. Martins Tostes², A. Massafferri¹, R. Matev³⁵, Z. Mathe³⁵, C. Matteuzzi²⁰, M. Matveev²⁷, E. Maurice⁶, A. Mazurov^{16,30,35,e}, J. McCarthy⁴², R. McNulty¹², B. Meadows⁵⁷, M. Meissner¹¹, M. Merk³⁸, D.A. Milanes¹³, M.-N. Minard⁴, J. Molina Rodriguez⁵⁴, S. Monteil⁵, D. Moran⁵¹, P. Morawski²³, R. Mountain⁵³, I. Mous³⁸, F. Muheim⁴⁷, K. Müller³⁷, R. Muresan²⁶, B. Muryn²⁴, B. Muster³⁶, P. Naik⁴³, T. Nakada³⁶, R. Nandakumar⁴⁶, I. Nasteva¹, M. Needham⁴⁷, N. Neufeld³⁵, A.D. Nguyen³⁶, T.D. Nguyen³⁶, C. Nguyen-Mau^{36,o}, M. Nicol⁷, V. Niess⁵, N. Nikitin²⁹, T. Nikodem¹¹, S. Nisar⁵⁶, A. Nomerotski^{52,35}, A. Novoselov³², A. Oblakowska-Mucha²⁴, V. Obraztsov³², S. Oggero³⁸, S. Ogilvy⁴⁸, O. Okhrimenko⁴¹, R. Oldeman^{15,d,35}, M. Orlandea²⁶, J.M. Otalora Goicochea², P. Owen⁵⁰, B.K. Pal⁵³, A. Palano^{13,b}, M. Palutan¹⁸, J. Panman³⁵, A. Papanestis⁴⁶, M. Pappagallo⁴⁸, C. Parkes⁵¹, C.J. Parkinson⁵⁰, G. Passaleva¹⁷, G.D. Patel⁴⁹, M. Patel⁵⁰, G.N. Patrick⁴⁶, C. Patrignani^{19,i}, C. Pavel-Nicorescu²⁶, A. Pazos Alvarez³⁴, A. Pellegrino³⁸, G. Penso^{22,l}, M. Pepe Altarelli³⁵, S. Perazzini^{14,c}, D.L. Perego^{20,j}, E. Perez Trigo³⁴, A. Pérez-Calero Yzquierdo³³, P. Perret⁵, M. Perrin-Terrin⁶, G. Pessina²⁰, K. Petridis⁵⁰, A. Petrolini^{19,i}, A. Phan⁵³, E. Picatoste Olloqui³³, B. Pietrzyk⁴, T. Pilar⁴⁵, D. Pinci²², S. Playfer⁴⁷, M. Plo Casasus³⁴, F. Polci⁸, G. Polok²³, A. Poluektov^{45,31}, E. Polcarpo², D. Popov¹⁰, B. Popovici²⁶, C. Potterat³³, A. Powell⁵², J. Prisciandaro³⁶, V. Pugatch⁴¹, A. Puig Navarro³⁶, W. Qian⁴, J.H. Rademacker⁴³, B. Rakotomiamanana³⁶, M.S. Rangel², I. Raniuk², N. Rauschmayr³⁵, G. Raven³⁹, S. Redford⁵², M.M. Reid⁴⁵, A.C. dos Reis¹, S. Ricciardi⁴⁶, A. Richards⁵⁰, K. Rinnert⁴⁹, V. Rives Molina³³, D.A. Roa Romero⁵, P. Robbe⁷, E. Rodrigues^{51,48}, P. Rodriguez Perez³⁴, G.J. Rogers⁴⁴, S. Roiser³⁵, V. Romanovsky³², A. Romero Vidal³⁴, J. Rouvinet³⁶, T. Ruf³⁵, H. Ruiz³³, G. Sabatino^{22,k}, J.J. Saborido Silva³⁴, N. Sagidova²⁷, P. Sail⁴⁸, B. Saitta^{15,d}, C. Salzmann³⁷, B. Sanmartin Sedes³⁴, M. Sannino^{19,i}, R. Santacesaria²², C. Santamarina Rios³⁴, E. Santovetti^{21,k}, M. Sapunov⁶, A. Sarti^{18,l}, C. Satriano^{22,m}, A. Satta²¹, M. Savrie^{16,e}, P. Schaack⁵⁰, M. Schiller³⁹, H. Schindler³⁵, S. Schleich⁹, M. Schlupp⁹, M. Schmelling¹⁰, B. Schmidt³⁵, O. Schneider³⁶, A. Schopper³⁵, M.-H. Schune⁷, R. Schwemmer³⁵, B. Sciascia¹⁸, A. Sciubba^{18,l}, M. Seco³⁴, A. Semennikov²⁸, K. Senderowska²⁴, I. Sepp⁵⁰, N. Serra³⁷, J. Serrano⁶, P. Seyfert¹¹, M. Shapkin³², I. Shapoval^{40,35}, P. Shatalov²⁸, Y. Shcheglov²⁷, T. Shears^{49,35}, L. Shekhtman³¹, O. Shevchenko⁴⁰, V. Shevchenko²⁸, A. Shires⁵⁰, R. Silva Coutinho⁴⁵, T. Skwarnicki⁵³, N.A. Smith⁴⁹, E. Smith^{52,46}, M. Smith⁵¹, K. Sobczak⁵, M.D. Sokoloff⁵⁷, F.J.P. Soler⁴⁸, F. Soomro^{18,35}, D. Souza⁴³, B. Souza De Paula², B. Spaan⁹, A. Sparkes⁴⁷, P. Spradlin⁴⁸, F. Stagni³⁵, S. Stahl¹¹, O. Steinkamp³⁷, S. Stoica²⁶, S. Stone⁵³, B. Storaci³⁸, M. Straticiu²⁶, U. Straumann³⁷, V.K. Subbiah³⁵, S. Swientek⁹, M. Szczekowski²⁵, P. Szczypka^{36,35}, T. Szumlak²⁴, S. T'Jampens⁴, M. Teklishyn⁷, E. Teodorescu²⁶, F. Teubert³⁵, C. Thomas⁵², E. Thomas³⁵, J. van Tilburg¹¹, V. Tisserand⁴, M. Tobin³⁷, S. Tolk³⁹, D. Tonelli³⁵, S. Topp-Joergensen⁵², N. Torr⁵², E. Tournefier^{4,50}, S. Tourneur³⁶, M.T. Tran³⁶, M. Tresch³⁷, A. Tsaregorodtsev⁶, P. Tsopelas³⁸, N. Tuning³⁸, M. Ubeda Garcia³⁵, A. Ukleja²⁵, D. Urner⁵¹, U. Uwer¹¹, V. Vagnoni¹⁴, G. Valenti¹⁴, R. Vazquez Gomez³³, P. Vazquez Regueiro³⁴, S. Vecchi¹⁶, J.J. Velthuis⁴³, M. Veltri^{17,g}, G. Veneziano³⁶, M. Vesterinen³⁵, B. Viaud⁷, D. Vieira², X. Vilasis-Cardona^{33,n}, A. Vollhardt³⁷, D. Volyanskyy¹⁰, D. Voong⁴³, A. Vorobyev²⁷, V. Vorobyev³¹, C. Voß⁵⁵, H. Voss¹⁰, R. Waldi⁵⁵, R. Wallace¹², S. Wandernoth¹¹, J. Wang⁵³, D.R. Ward⁴⁴, N.K. Watson⁴², A.D. Webber⁵¹, D. Websdale⁵⁰, M. Whitehead⁴⁵, J. Wicht³⁵, D. Wiedner¹¹, L. Wiggers³⁸, G. Wilkinson⁵², M.P. Williams^{45,46}, M. Williams^{50,p}, F.F. Wilson⁴⁶, J. Wishahi⁹, M. Witek²³, W. Witzeling³⁵, S.A. Wotton⁴⁴, S. Wright⁴⁴, S. Wu³, K. Wyllie³⁵, Y. Xie^{47,35}, F. Xing⁵², Z. Xing⁵³, Z. Yang³, R. Young⁴⁷, X. Yuan³, O. Yushchenko³², M. Zangoli¹⁴, M. Zavertyaev^{10,a}, F. Zhang³, L. Zhang⁵³, W.C. Zhang¹², Y. Zhang³, A. Zhelezov¹¹, L. Zhong³, A. Zvyagin³⁵.

¹ Centro Brasileiro de Pesquisas Físicas (CBPF), Rio de Janeiro, Brazil

² Universidade Federal do Rio de Janeiro (UFRJ), Rio de Janeiro, Brazil

³ Center for High Energy Physics, Tsinghua University, Beijing, China

⁴ LAPP, Université de Savoie, CNRS/IN2P3, Annecy-Le-Vieux, France

⁵ Clermont Université, Université Blaise Pascal, CNRS/IN2P3, LPC, Clermont-Ferrand, France

⁶ CPPM, Aix-Marseille Université, CNRS/IN2P3, Marseille, France

⁷ LAL, Université Paris-Sud, CNRS/IN2P3, Orsay, France

⁸ LPNHE, Université Pierre et Marie Curie, Université Paris Diderot, CNRS/IN2P3, Paris, France

⁹ Fakultät Physik, Technische Universität Dortmund, Dortmund, Germany

¹⁰ Max-Planck-Institut für Kernphysik (MPIK), Heidelberg, Germany

¹¹ Physikalisches Institut, Ruprecht-Karls-Universität Heidelberg, Heidelberg, Germany

¹² School of Physics, University College Dublin, Dublin, Ireland

¹³ Sezione INFN di Bari, Bari, Italy

¹⁴ Sezione INFN di Bologna, Bologna, Italy

¹⁵ Sezione INFN di Cagliari, Cagliari, Italy

¹⁶ Sezione INFN di Ferrara, Ferrara, Italy

¹⁷ Sezione INFN di Firenze, Firenze, Italy

¹⁸ Laboratori Nazionali dell'INFN di Frascati, Frascati, Italy

¹⁹ Sezione INFN di Genova, Genova, Italy

²⁰ Sezione INFN di Milano Bicocca, Milano, Italy

²¹ Sezione INFN di Roma Tor Vergata, Roma, Italy

²² Sezione INFN di Roma La Sapienza, Roma, Italy

²³ Henryk Niewodniczanski Institute of Nuclear Physics Polish Academy of Sciences, Kraków, Poland

²⁴ AGH University of Science and Technology, Kraków, Poland

²⁵ National Center for Nuclear Research (NCBJ), Warsaw, Poland

²⁶ Horia Hulubei National Institute of Physics and Nuclear Engineering, Bucharest-Magurele, Romania

- ²⁷ Petersburg Nuclear Physics Institute (PNPI), Gatchina, Russia
²⁸ Institute of Theoretical and Experimental Physics (ITEP), Moscow, Russia
²⁹ Institute of Nuclear Physics, Moscow State University (SINP MSU), Moscow, Russia
³⁰ Institute for Nuclear Research of the Russian Academy of Sciences (INR RAN), Moscow, Russia
³¹ Budker Institute of Nuclear Physics (SB RAS) and Novosibirsk State University, Novosibirsk, Russia
³² Institute for High Energy Physics (IHEP), Protvino, Russia
³³ Universitat de Barcelona, Barcelona, Spain
³⁴ Universidad de Santiago de Compostela, Santiago de Compostela, Spain
³⁵ European Organization for Nuclear Research (CERN), Geneva, Switzerland
³⁶ Ecole Polytechnique Fédérale de Lausanne (EPFL), Lausanne, Switzerland
³⁷ Physik-Institut, Universität Zürich, Zürich, Switzerland
³⁸ Nikhef National Institute for Subatomic Physics, Amsterdam, The Netherlands
³⁹ Nikhef National Institute for Subatomic Physics and VU University Amsterdam, Amsterdam, The Netherlands
⁴⁰ NSC Kharkiv Institute of Physics and Technology (NSC KIPT), Kharkiv, Ukraine
⁴¹ Institute for Nuclear Research of the National Academy of Sciences (KINR), Kyiv, Ukraine
⁴² University of Birmingham, Birmingham, United Kingdom
⁴³ H.H. Wills Physics Laboratory, University of Bristol, Bristol, United Kingdom
⁴⁴ Cavendish Laboratory, University of Cambridge, Cambridge, United Kingdom
⁴⁵ Department of Physics, University of Warwick, Coventry, United Kingdom
⁴⁶ STFC Rutherford Appleton Laboratory, Didcot, United Kingdom
⁴⁷ School of Physics and Astronomy, University of Edinburgh, Edinburgh, United Kingdom
⁴⁸ School of Physics and Astronomy, University of Glasgow, Glasgow, United Kingdom
⁴⁹ Oliver Lodge Laboratory, University of Liverpool, Liverpool, United Kingdom
⁵⁰ Imperial College London, London, United Kingdom
⁵¹ School of Physics and Astronomy, University of Manchester, Manchester, United Kingdom
⁵² Department of Physics, University of Oxford, Oxford, United Kingdom
⁵³ Syracuse University, Syracuse, NY, United States
⁵⁴ Pontifícia Universidade Católica do Rio de Janeiro (PUC-Rio), Rio de Janeiro, Brazil, associated to ²
⁵⁵ Institut für Physik, Universität Rostock, Rostock, Germany, associated to ¹¹
⁵⁶ Institute of Information Technology, COMSATS, Lahore, Pakistan, associated to ⁵³
⁵⁷ University of Cincinnati, Cincinnati, OH, United States, associated to ⁵³

^a P.N. Lebedev Physical Institute, Russian Academy of Science (LPI RAS), Moscow, Russia

^b Università di Bari, Bari, Italy

^c Università di Bologna, Bologna, Italy

^d Università di Cagliari, Cagliari, Italy

^e Università di Ferrara, Ferrara, Italy

^f Università di Firenze, Firenze, Italy

^g Università di Urbino, Urbino, Italy

^h Università di Modena e Reggio Emilia, Modena, Italy

ⁱ Università di Genova, Genova, Italy

^j Università di Milano Bicocca, Milano, Italy

^k Università di Roma Tor Vergata, Roma, Italy

^l Università di Roma La Sapienza, Roma, Italy

^m Università della Basilicata, Potenza, Italy

ⁿ LIFAELS, La Salle, Universitat Ramon Llull, Barcelona, Spain

^o Hanoi University of Science, Hanoi, Viet Nam

^p Massachusetts Institute of Technology, Cambridge, MA, United States

A search for the rare decays $B_s^0 \rightarrow \mu^+\mu^-$ and $B^0 \rightarrow \mu^+\mu^-$ is performed using data collected in 2011 and 2012 with the LHCb experiment at the Large Hadron Collider. The data samples comprise 1.1 fb^{-1} of proton-proton collisions at $\sqrt{s} = 8 \text{ TeV}$ and 1.0 fb^{-1} at $\sqrt{s} = 7 \text{ TeV}$. We observe an excess of $B_s^0 \rightarrow \mu^+\mu^-$ candidates with respect to the background expectation. The probability that the background could produce such an excess or larger is 5.3×10^{-4} corresponding to a signal significance of 3.5 standard deviations. A maximum-likelihood fit gives a branching fraction of $\mathcal{B}(B_s^0 \rightarrow \mu^+\mu^-) = (3.2_{-1.2}^{+1.5}) \times 10^{-9}$, where the statistical uncertainty is 95% of the total uncertainty. This result is in agreement with the Standard Model expectation. The observed number of $B^0 \rightarrow \mu^+\mu^-$ candidates is consistent with the background expectation, giving an upper limit of $\mathcal{B}(B^0 \rightarrow \mu^+\mu^-) < 9.4 \times 10^{-10}$ at 95% confidence level.

Submitted to Physical Review Letters

The rare decays $B_s^0 \rightarrow \mu^+\mu^-$ and $B^0 \rightarrow \mu^+\mu^-$ are highly suppressed in the Standard Model (SM). Precise predictions of their branching fractions, $\mathcal{B}(B_s^0 \rightarrow \mu^+\mu^-) = (3.23 \pm 0.27) \times 10^{-9}$ and $\mathcal{B}(B^0 \rightarrow \mu^+\mu^-) = (1.07 \pm 0.10) \times 10^{-10}$ [1] make these modes powerful probes in the search for deviations from the SM, especially in models with a non-standard Higgs sector. Taking the measured finite width difference of the B_s^0 system [2] into account [3], the time integrated branching fraction of $B_s^0 \rightarrow \mu^+\mu^-$ that should be compared to the experimental value is $(3.54 \pm 0.30) \times 10^{-9}$.

Previous searches [4–8] already constrain possible deviations from the SM predictions. The lowest published limits are $\mathcal{B}(B_s^0 \rightarrow \mu^+\mu^-) < 4.5 \times 10^{-9}$ and $\mathcal{B}(B^0 \rightarrow \mu^+\mu^-) < 1.0 \times 10^{-9}$ at 95% confidence level (CL) from the LHCb collaboration using 1.0 fb^{-1} of data collected in pp collisions in 2011 at $\sqrt{s} = 7 \text{ TeV}$ [8]. This Letter reports an update of this search with 1.1 fb^{-1} of data recorded in 2012 at $\sqrt{s} = 8 \text{ TeV}$.

The analysis of 2012 data is similar to that described in Ref. [8] with two main improvements: the use of particle identification to select $B_{(s)}^0 \rightarrow h^+h'^-$ (with $h^{(\prime)} = K, \pi$) decays used to calibrate the geometrical and kinematic variables, and a refined estimate of the exclusive backgrounds. To avoid potential bias, the events in the signal region were not examined until all the analysis choices were finalized. The updated estimate of the exclusive backgrounds is also applied to the 2011 data [8] and the results re-evaluated. The results obtained with the combined 2011 and 2012 datasets supersede those of Ref. [8].

The LHCb detector is a single-arm forward spectrometer covering the pseudorapidity range $2 < \eta < 5$, and is described in detail in Ref. [9]. The simulated events used in this analysis are produced using the software described in Refs. [10–16].

Candidate $B_{(s)}^0 \rightarrow \mu^+\mu^-$ events are required to be selected by a hardware and a subsequent software trigger. The candidates are predominantly selected by single and dimuon triggers [17] and, to a smaller extent, by a generic b -hadron trigger [18]. Candidate events in the $B^+ \rightarrow J/\psi K^+$ control channel, with $J/\psi \rightarrow \mu^+\mu^-$ (inclusion of charged conjugated processes is implied throughout

this Letter), are selected in a very similar way, the only difference being a different dimuon mass requirement in the final software trigger. The $B_{(s)}^0 \rightarrow h^+h'^-$ decays are predominantly selected by a hardware trigger based on the calorimeter transverse energy and subsequently by a generic b -hadron software trigger.

The $B_{(s)}^0 \rightarrow \mu^+\mu^-$ candidates are selected by requiring two high quality muon candidates [19] displaced with respect to any pp interaction vertex (primary vertex, PV), and forming a secondary vertex (SV) with a χ^2 per degree of freedom smaller than 9 and separated from the PV in the downstream direction by a flight distance significance greater than 15. Only candidates with an impact parameter χ^2 , $\text{IP}\chi^2$ (defined as the difference between the χ^2 of the PV formed with and without the considered tracks) less than 25 are considered. When more than one PV is reconstructed, that giving the smallest $\text{IP}\chi^2$ for the B candidate is chosen. Tracks from selected candidates are required to have transverse momentum p_T satisfying $0.25 < p_T < 40 \text{ GeV}/c$ and $p < 500 \text{ GeV}/c$. Only B candidates with decay times smaller than $9\tau(B_s^0)$ [20] and with invariant mass in the range [4900, 6000] MeV/c^2 are kept.

Dimuon candidates from elastic diphoton production are heavily suppressed by requiring $p_T(B) > 0.5 \text{ GeV}/c$. The surviving background comprises mainly random combinations of muons from semileptonic decays of two different b hadrons ($b\bar{b} \rightarrow \mu^+\mu^-X$, where X is any other set of particles).

Two channels, $B^+ \rightarrow J/\psi K^+$ and $B^0 \rightarrow K^+\pi^-$, serve as normalization modes. The first mode has trigger and muon identification efficiencies similar to those of the signal, but a different number of tracks in the final state. The second mode has a similar topology, but is triggered differently. The selection of these channels is as close as possible to that of the signal to reduce the impact of potential systematic uncertainties.

The $B^0 \rightarrow K^+\pi^-$ selection is the same as for $B_{(s)}^0 \rightarrow \mu^+\mu^-$ signal except for muon identification. The two tracks are nevertheless required to be within the muon detector acceptance.

The $J/\psi \rightarrow \mu^+\mu^-$ decay in the $B^+ \rightarrow J/\psi K^+$

normalization channel is also selected similarly to the $B_{(s)}^0 \rightarrow \mu^+\mu^-$ signals, except for the requirements on the $\text{IP}\chi^2$ and mass. Kaon candidates are required to have $\text{IP}\chi^2 > 25$.

A two-stage multivariate selection, based on boosted decision trees [21, 22] is applied to the $B_{(s)}^0 \rightarrow \mu^+\mu^-$ candidates. A cut on the first multivariate discriminant, unchanged from Ref. [8], removes 80 % of the background while retaining 92 % of signal. The efficiencies of this cut for the signal and the normalization samples are equal within 0.2 % as determined from simulation.

The output of the second multivariate discriminant, called BDT, and the dimuon invariant mass are used to classify the selected candidates. The nine variables entering the BDT are the B candidate IP, the minimum $\text{IP}\chi^2$ of the two muons with respect to any PV, the sum of the degrees of isolation of the muons (the number of good two-track vertices a muon can make with other tracks in the event), the B candidate decay time, p_{T} , and isolation [23], the distance of closest approach between the two muons, the minimum p_{T} of the muons, and the cosine of the angle between the muon momentum in the dimuon rest frame and the vector perpendicular to both the B candidate momentum and the beam axis.

The BDT discriminant is trained using simulated samples consisting of $B_s^0 \rightarrow \mu^+\mu^-$ for signal and $b\bar{b} \rightarrow \mu^+\mu^-X$ for background. The BDT response is defined such that it is approximately uniformly distributed between zero and one for signal events and peaks at zero for the background. The BDT response is independent of the invariant mass for signal inside the search window. The probability for a $B_{(s)}^0 \rightarrow \mu^+\mu^-$ event to have a given BDT value is obtained from data using $B^0 \rightarrow K^+\pi^-$, $\pi^+\pi^-$ and $B_s^0 \rightarrow \pi^+K^-$, K^+K^- exclusive decays selected as the signal events and triggered independently of the tracks from $B_{(s)}^0$ candidates.

The invariant mass lineshape of the signal events is described by a Crystal Ball function [24]. The peak values for the B_s^0 and B^0 mesons, $m_{B_s^0}$ and m_{B^0} , are obtained from the $B_s^0 \rightarrow K^+K^-$ and $B^0 \rightarrow K^+\pi^-$, $B^0 \rightarrow \pi^+\pi^-$ samples. The resolutions are determined by combining the results obtained with a power-law interpolation between the measured resolutions of charmonium and bottomonium resonances decaying into two muons with those obtained with a fit of the mass distributions of $B^0 \rightarrow K^+\pi^-$, $B^0 \rightarrow \pi^+\pi^-$ and $B_s^0 \rightarrow K^+K^-$ samples. The results are $\sigma_{B_s^0} = 25.0 \pm 0.4 \text{ MeV}/c^2$ and $\sigma_{B^0} = 24.6 \pm 0.4 \text{ MeV}/c^2$, respectively. The transition point of the radiative tail is obtained from simulated $B_s^0 \rightarrow \mu^+\mu^-$ events smeared to reproduce the mass resolution measured in data.

The $B_s^0 \rightarrow \mu^+\mu^-$ and $B^0 \rightarrow \mu^+\mu^-$ yields are translated

into branching fractions using

$$\begin{aligned} \mathcal{B}(B_{(s)}^0 \rightarrow \mu^+\mu^-) &= \frac{\mathcal{B}_{\text{norm}} \epsilon_{\text{norm}} f_{\text{norm}}}{N_{\text{norm}} \epsilon_{\text{sig}} f_{d(s)}} \times N_{B_{(s)}^0 \rightarrow \mu^+\mu^-} \\ &= \alpha_{B_{(s)}^0 \rightarrow \mu^+\mu^-}^{\text{norm}} \times N_{B_{(s)}^0 \rightarrow \mu^+\mu^-}, \end{aligned} \quad (1)$$

where $\mathcal{B}_{\text{norm}}$ represents the branching fraction, N_{norm} the number of signal events in the normalization channel obtained from a fit to the invariant mass distribution, and $N_{B_{(s)}^0 \rightarrow \mu^+\mu^-}$ is the number of observed signal events.

The factors $f_{d(s)}$ and f_{norm} indicate the probabilities that a b quark fragments into a $B_{(s)}^0$ meson and into the hadron involved in the given normalization mode, respectively. We assume $f_d = f_u$ and use $f_s/f_d = 0.256 \pm 0.020$ measured in pp collision data at $\sqrt{s} = 7 \text{ TeV}$ [25]. This value is in agreement within 1.5σ with that found at $\sqrt{s} = 8 \text{ TeV}$ by comparing the ratios of the yields of $B_s^0 \rightarrow J/\psi\phi$ and $B^+ \rightarrow J/\psi K^+$ decays. The measured dependence of f_s/f_d on $p_{\text{T}}(B)$ [25] is found to be negligible for this analysis.

The efficiency $\epsilon_{\text{sig(norm)}}$ for the signal (normalization channel) is the product of the reconstruction efficiency of the final state particles including the geometric detector acceptance, the selection efficiency and the trigger efficiency. The ratio of acceptance, reconstruction and selection efficiencies is computed using simulation. Potential differences between data and simulation are accounted for as systematic uncertainties. Reweighting techniques are used for all the distributions in the simulation that do not match those from data. The trigger efficiency is evaluated with data-driven techniques [26]. The observed numbers of $B^+ \rightarrow J/\psi K^+$ and $B^0 \rightarrow K^+\pi^-$ candidates in the 2012 dataset are $424\,200 \pm 1500$ and $14\,600 \pm 1100$, respectively. The two normalization factors $\alpha_{B_{(s)}^0 \rightarrow \mu^+\mu^-}^{\text{norm}}$ are in agreement within the uncertainties, and their weighted average, taking correlations into account, gives $\alpha_{B_s^0 \rightarrow \mu^+\mu^-} = (2.52 \pm 0.23) \times 10^{-10}$ and $\alpha_{B^0 \rightarrow \mu^+\mu^-} = (6.45 \pm 0.30) \times 10^{-11}$.

In total, 24044 muon pairs with invariant mass between 4900 and 6000 MeV/c^2 pass the trigger and selection requirements. Given the measured normalization factors and assuming the SM branching fractions, the data sample is expected to contain about 14.1 $B_s^0 \rightarrow \mu^+\mu^-$ and 1.7 $B^0 \rightarrow \mu^+\mu^-$ decays.

The BDT range is divided into eight bins with boundaries [0.0, 0.25, 0.4, 0.5, 0.6, 0.7, 0.8, 0.9, 1.0]. For the 2012 dataset, only one bin is considered in the BDT range 0.8–1.0 due to the lack of events in the mass sidebands for $\text{BDT} > 0.9$. The signal regions are defined by $m_{B_{(s)}^0} \pm 60 \text{ MeV}/c^2$.

The expected number of combinatorial background events is determined by interpolating from the invariant mass sideband regions defined as $[4900 \text{ MeV}/c^2, m_{B^0} - 60 \text{ MeV}/c^2]$ and $[m_{B_s^0} + 60 \text{ MeV}/c^2, 6000 \text{ MeV}/c^2]$. The low-mass sideband and the B^0 and B_s^0 signal regions

are potentially polluted by exclusive backgrounds with or without misidentification of the muon candidates.

The first category includes $B^0 \rightarrow \pi^- \mu^+ \nu_\mu$, $B_{(s)}^0 \rightarrow h^+ h'^-$, $B_s^0 \rightarrow K^- \mu^+ \nu_\mu$ and $\Lambda_b^0 \rightarrow p \mu^- \bar{\nu}_\mu$ decays. The $B^0 \rightarrow \pi^- \mu^+ \nu_\mu$ and $B_{(s)}^0 \rightarrow h^+ h'^-$ branching fractions are taken from Ref. [20]. The theoretical estimates of the $\Lambda_b^0 \rightarrow p \mu^- \bar{\nu}_\mu$ and $B_s^0 \rightarrow K^- \mu^+ \nu_\mu$ branching fractions are taken from Refs. [27] and [28], respectively. The mass and BDT distributions of these modes are evaluated from simulated samples where the $K \rightarrow \mu$, $\pi \rightarrow \mu$ and $p \rightarrow \mu$ misidentification probabilities as a function of momentum and transverse momentum are those determined from $D^{*+} \rightarrow D^0 \pi^+$, $D^0 \rightarrow K^- \pi^+$ and $\Lambda \rightarrow p \pi^-$ data samples. We use the Λ_b^0 fragmentation fraction $f_{\Lambda_b^0}$ measured by LHCb [29] and account for its p_T dependence.

The second category includes $B_c^+ \rightarrow J/\psi(\mu^+ \mu^-) \mu^+ \nu_\mu$, $B_s^0 \rightarrow \mu^+ \mu^- \gamma$ and $B^{0(+)} \rightarrow \pi^{0(+)} \mu^+ \mu^-$ decays, evaluated assuming branching fraction values from Refs. [30], [31] and [32], respectively. Apart from $B_{(s)}^0 \rightarrow h^+ h'^-$, all background modes are normalized relative to the $B^+ \rightarrow J/\psi K^+$ decay. The $B^0 \rightarrow \pi^- \mu^+ \nu_\mu$, $B_{(s)}^0 \rightarrow h^+ h'^-$ and $B^{0(+)} \rightarrow \pi^{0(+)} \mu^+ \mu^-$ decays are the dominant exclusive modes in the range $\text{BDT} > 0.8$, which accounts for 70% of the sensitivity.

In the full BDT range, 8.6 ± 0.7 doubly misidentified $B_{(s)}^0 \rightarrow h^+ h'^-$ decays are expected in the full mass interval, $4.1_{-0.8}^{+1.7}$ in the B^0 and $0.76_{-0.18}^{+0.26}$ in the B_s^0 signal region. The expected yields for $B^0 \rightarrow \pi^- \mu^+ \nu_\mu$ and $B^{0(+)} \rightarrow \pi^{0(+)} \mu^+ \mu^-$ are 41.1 ± 0.4 and 11.9 ± 3.5 , respectively, in the full mass and BDT ranges. The contributions of these two backgrounds above $m_{B^0} - 60 \text{ MeV}/c^2$ are negligible. The fractions of these backgrounds with $\text{BDT} > 0.8$, in the full mass range, are $(19.0 \pm 1.4)\%$, $(11.1 \pm 0.5)\%$, and $(12.2 \pm 0.3)\%$ for $B_{(s)}^0 \rightarrow h^+ h'^-$, $B^0 \rightarrow \pi^- \mu^+ \nu_\mu$ and $B^{0(+)} \rightarrow \pi^{0(+)} \mu^+ \mu^-$ decays, respectively.

A simultaneous unbinned maximum-likelihood fit to the mass projections in the BDT bins is performed on the mass sidebands to determine the number of expected combinatorial background events in the B^0 and B_s^0 signal regions used in the derivation of the branching fraction limit. In this fit the parameters that describe the mass distributions of the exclusive backgrounds, their fractional yields in each BDT bin and their overall yields are limited by Gaussian constraints according to their expected values and uncertainties. The combinatorial background is parameterized with an exponential function with slope and normalization allowed to vary. The systematic uncertainty on the estimated number of combinatorial background events in the signal regions is determined by fluctuating the number of events observed in the sidebands according to a Poisson distribution, and by varying the exponential slope according to its uncer-

tainty. The same fit is then performed on the full mass range to determine the $B_s^0 \rightarrow \mu^+ \mu^-$ and $B^0 \rightarrow \mu^+ \mu^-$ branching fractions, which are free parameters of the fit. The $B_s^0 \rightarrow \mu^+ \mu^-$ and $B^0 \rightarrow \mu^+ \mu^-$ fractional yields in BDT bins are constrained to the BDT fractions calibrated with the $B_{(s)}^0 \rightarrow h^+ h'^-$ sample. The parameters of the Crystal Ball functions that describe the mass line-shapes and the normalization factors are restricted by Gaussian constraints according to their expected values and uncertainties.

The compatibility of the observed distribution of events with that expected for a given branching fraction hypothesis is computed using the CL_s method [33]. The method provides CL_{s+b} , a measure of the compatibility of the observed distribution with the signal plus background hypothesis, CL_b , a measure of the compatibility with the background-only hypothesis, and $\text{CL}_s = \text{CL}_{s+b}/\text{CL}_b$.

The invariant mass signal regions are divided into nine bins with boundaries $m_{B_{(s)}^0} \pm 18, 30, 36, 48, 60 \text{ MeV}/c^2$. In each bin of the two-dimensional space formed by the dimuon mass and the BDT output we count the number of observed candidates, and compute the expected number of signal and background events.

The comparison of the distributions of observed events and expected background events in the 2012 dataset results in p-values $(1 - \text{CL}_b)$ of 9×10^{-4} for the $B_s^0 \rightarrow \mu^+ \mu^-$ and 0.16 for the $B^0 \rightarrow \mu^+ \mu^-$ decay, computed at the branching fraction values corresponding to $\text{CL}_{s+b} = 0.5$. We observe an excess of $B_s^0 \rightarrow \mu^+ \mu^-$ candidates with respect to background expectation with a significance of 3.3 standard deviations. The simultaneous unbinned maximum-likelihood fit gives $\mathcal{B}(B_s^0 \rightarrow \mu^+ \mu^-) = (5.1_{-1.9}^{+2.3}(\text{stat})_{-0.4}^{+0.7}(\text{syst})) \times 10^{-9}$. The statistical uncertainty reflects the interval corresponding to a change of 0.5 with respect to the maximum of the likelihood after fixing all the fit parameters to their expected values except the $B_s^0 \rightarrow \mu^+ \mu^-$ and $B^0 \rightarrow \mu^+ \mu^-$ branching fractions and the slope and normalization of the combinatorial background. The systematic uncertainty is obtained by subtracting in quadrature the statistical uncertainty from the total uncertainty obtained from the likelihood with all nuisance parameters left to vary according to their uncertainties. An additional systematic uncertainty of 0.16×10^{-9} reflects the impact on the result of the change in the parameterization of the combinatorial background from a single to a double exponential, and is added in quadrature.

The expected and measured limits on the $B^0 \rightarrow \mu^+ \mu^-$ branching fraction at 90% and 95% CL are shown in Table I. The expected limits are computed allowing for the presence of $B_{(s)}^0 \rightarrow \mu^+ \mu^-$ events according to the SM branching fractions, including cross-feed between the two modes.

The contribution of the exclusive background compo-

TABLE I. Expected and observed limits on the $B^0 \rightarrow \mu^+\mu^-$ branching fractions for the 2012 and for the combined 2011+2012 datasets.

Dataset	Limit at	90 % CL	95 % CL
2012	Exp. bkg+SM	8.5×10^{-10}	10.5×10^{-10}
	Exp. bkg	7.6×10^{-10}	9.6×10^{-10}
	Observed	10.5×10^{-10}	12.5×10^{-10}
2011+2012	Exp. bkg+SM	5.8×10^{-10}	7.1×10^{-10}
	Exp. bkg	5.0×10^{-10}	6.0×10^{-10}
	Observed	8.0×10^{-10}	9.4×10^{-10}

nents is also evaluated for the 2011 dataset, modifying the number of expected combinatorial background in the signal regions. The results for the $B_{(s)}^0 \rightarrow \mu^+\mu^-$ branching fractions have been updated accordingly. We obtain $\mathcal{B}(B_s^0 \rightarrow \mu^+\mu^-) < 5.1 \times 10^{-9}$ and $\mathcal{B}(B^0 \rightarrow \mu^+\mu^-) < 13 \times 10^{-10}$ at 95 % CL to be compared to the published limits $\mathcal{B}(B_s^0 \rightarrow \mu^+\mu^-) < 4.5 \times 10^{-9}$ and $\mathcal{B}(B^0 \rightarrow \mu^+\mu^-) < 10.3 \times 10^{-10}$ at 95 % CL [8], respectively. The $(1-\text{CL}_b)$ p-value for $B_s^0 \rightarrow \mu^+\mu^-$ changes from 18 % to 11 % and the $B_s^0 \rightarrow \mu^+\mu^-$ branching fraction increases by $\sim 0.3\sigma$ from $(0.8_{-1.3}^{+1.8}) \times 10^{-9}$ to $(1.4_{-1.3}^{+1.7}) \times 10^{-9}$. This shift is compatible with the systematic uncertainty previously assigned to the background shape [8]. The values of the $B_s^0 \rightarrow \mu^+\mu^-$ branching fraction obtained with the 2011 and 2012 datasets are compatible within 1.5σ .

The 2011 and 2012 results are combined by computing the CL_s and performing the maximum-likelihood fit simultaneously to the eight and seven BDT bins of the 2011 and 2012 datasets, respectively. The parameters that are considered 100 % correlated between the two datasets are f_s/f_d , $\mathcal{B}(B^+ \rightarrow J/\psi K^+)$ and $\mathcal{B}(B^0 \rightarrow K^+\pi^-)$, the transition point of the Crystal Ball function describing the signal mass lineshape, the mass distribution of the $B_{(s)}^0 \rightarrow h^+h'^-$ background, the BDT and mass distributions of the $B^0 \rightarrow \pi^-\mu^+\nu_\mu$ and $B^{0(+)} \rightarrow \pi^{0(+)}\mu^+\mu^-$ backgrounds and the SM predictions of the $B_s^0 \rightarrow \mu^+\mu^-$ and $B^0 \rightarrow \mu^+\mu^-$ branching fractions. The distribution of the expected and observed events in bins of BDT in the signal regions obtained from the simultaneous analysis of the 2011 and 2012 datasets, are summarized in Table II.

The expected and observed upper limits for the $B^0 \rightarrow \mu^+\mu^-$ channel obtained from the combined 2011+2012 datasets are summarized in Table I and the expected and observed CL_s values as a function of the branching fraction are shown in Fig. 1. The observed CL_b value at $\text{CL}_{s+b} = 0.5$ is 89 %. The probability that background processes can produce the observed number of $B_s^0 \rightarrow \mu^+\mu^-$ candidates or more is 5×10^{-4} and corresponds to a statistical significance of 3.5σ . The value of the $B_s^0 \rightarrow \mu^+\mu^-$ branching fraction obtained from the fit

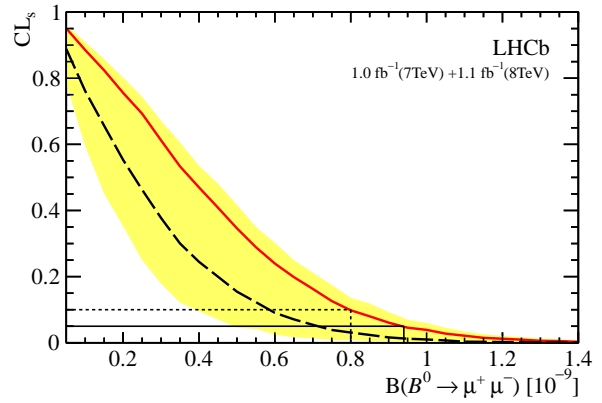


FIG. 1. CL_s as a function of the assumed $B^0 \rightarrow \mu^+\mu^-$ branching fraction for the combined 2011+2012 dataset. The dashed gray curve is the median of the expected CL_s distribution if background and SM signal were observed. The shaded yellow area covers, for each branching fraction value, 34 % of the expected CL_s distribution on each side of its median. The solid red curve is the observed CL_s .

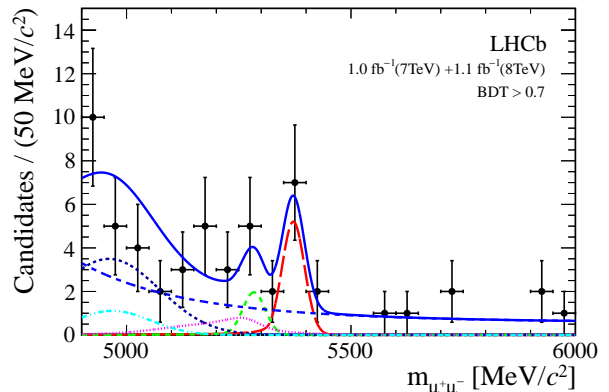


FIG. 2. Invariant mass distribution of the selected $B_s^0 \rightarrow \mu^+\mu^-$ candidates (black dots) with $\text{BDT} > 0.7$ in the combined 2011+2012 dataset. The result of the fit is overlaid (blue solid line) and the different components detailed: $B_s^0 \rightarrow \mu^+\mu^-$ (red long dashed), $B^0 \rightarrow \mu^+\mu^-$ (green medium dashed), $B_{(s)}^0 \rightarrow h^+h'^-$ (pink dotted), $B^0 \rightarrow \pi^-\mu^+\nu_\mu$ (black short dashed) and $B^{0(+)} \rightarrow \pi^{0(+)}\mu^+\mu^-$ (light blue dot dashed), and the combinatorial background (blue medium dashed).

is

$$\mathcal{B}(B_s^0 \rightarrow \mu^+\mu^-) = (3.2_{-1.2}^{+1.4}(\text{stat})_{-0.3}^{+0.5}(\text{syst})) \times 10^{-9}$$

and is in agreement with the SM expectation. The invariant mass distribution of the $B_{(s)}^0 \rightarrow \mu^+\mu^-$ candidates with $\text{BDT} > 0.7$ is shown in Fig. 2.

The true value of the $B_s^0 \rightarrow \mu^+\mu^-$ branching fraction is contained in the interval $[1.3, 5.8] \times 10^{-9}$ ($[1.1, 6.4] \times 10^{-9}$)

TABLE II. Expected combinatorial background, $B_{(s)}^0 \rightarrow h^+ h'^-$ peaking background, cross-feed, and signal events assuming the SM prediction, together with the number of observed candidates in the $B_s^0 \rightarrow \mu^+ \mu^-$ and $B^0 \rightarrow \mu^+ \mu^-$ mass signal regions, in bins of BDT for the 2011 (top) and for the 2012 (bottom) data samples. The quoted errors include statistical and systematic uncertainties.

Mode	BDT bin	0.0 – 0.25	0.25 – 0.4	0.4 – 0.5	0.5 – 0.6	0.6 – 0.7	0.7 – 0.8	0.8 – 0.9	0.9 – 1.0
$B_s^0 \rightarrow \mu^+ \mu^-$ (2011)	Exp. comb. bkg	1880_{-33}^{+33}	$55.5_{-2.9}^{+3.0}$	$12.1_{-1.3}^{+1.4}$	$4.16_{-0.79}^{+0.88}$	$1.81_{-0.51}^{+0.62}$	$0.77_{-0.38}^{+0.52}$	$0.47_{-0.36}^{+0.48}$	$0.24_{-0.20}^{+0.44}$
	Exp. peak. bkg	$0.13_{-0.05}^{+0.07}$	$0.07_{-0.02}^{+0.02}$	$0.05_{-0.02}^{+0.02}$	$0.05_{-0.01}^{+0.02}$	$0.05_{-0.01}^{+0.02}$	$0.05_{-0.01}^{+0.02}$	$0.05_{-0.01}^{+0.02}$	$0.05_{-0.01}^{+0.02}$
	Exp. signal	$2.70_{-0.80}^{+0.81}$	$1.30_{-0.23}^{+0.27}$	$1.03_{-0.17}^{+0.20}$	$0.92_{-0.13}^{+0.15}$	$1.06_{-0.15}^{+0.17}$	$1.10_{-0.15}^{+0.17}$	$1.26_{-0.17}^{+0.20}$	$1.31_{-0.25}^{+0.28}$
	Observed	1818	39	12	6	1	2	1	1
$B^0 \rightarrow \mu^+ \mu^-$ (2011)	Exp. comb. bkg	1995_{-34}^{+34}	$59.2_{-3.2}^{+3.3}$	$12.6_{-1.5}^{+1.6}$	$4.44_{-0.86}^{+0.99}$	$1.67_{-0.54}^{+0.66}$	$0.75_{-0.40}^{+0.58}$	$0.44_{-0.38}^{+0.57}$	$0.22_{-0.20}^{+0.48}$
	Exp. peak. bkg	$0.78_{-0.13}^{+0.38}$	$0.40_{-0.10}^{+0.14}$	$0.31_{-0.08}^{+0.11}$	$0.28_{-0.07}^{+0.09}$	$0.31_{-0.08}^{+0.10}$	$0.30_{-0.07}^{+0.10}$	$0.31_{-0.08}^{+0.10}$	$0.30_{-0.08}^{+0.11}$
	Exp. cross-feed	$0.43_{-0.13}^{+0.13}$	$0.21_{-0.03}^{+0.04}$	$0.16_{-0.02}^{+0.03}$	$0.15_{-0.02}^{+0.03}$	$0.17_{-0.03}^{+0.03}$	$0.17_{-0.02}^{+0.03}$	$0.20_{-0.02}^{+0.03}$	$0.21_{-0.03}^{+0.05}$
	Exp. signal	$0.33_{-0.10}^{+0.10}$	$0.16_{-0.03}^{+0.03}$	$0.13_{-0.02}^{+0.02}$	$0.11_{-0.02}^{+0.02}$	$0.13_{-0.02}^{+0.02}$	$0.13_{-0.02}^{+0.02}$	$0.15_{-0.02}^{+0.02}$	$0.16_{-0.03}^{+0.03}$
Observed	1904	50	20	5	2	1	4	1	
Mode	BDT bin	0.0 – 0.25	0.25 – 0.4	0.4 – 0.5	0.5 – 0.6	0.6 – 0.7	0.7 – 0.8	0.8–1.0	
$B_s^0 \rightarrow \mu^+ \mu^-$ (2012)	Exp. comb. bkg	2345_{-40}^{+40}	$56.7_{-2.9}^{+3.0}$	$13.1_{-1.4}^{+1.5}$	$4.42_{-0.81}^{+0.91}$	$2.10_{-0.56}^{+0.67}$	$0.35_{-0.22}^{+0.42}$	$0.39_{-0.21}^{+0.33}$	
	Exp. peak. bkg	$0.250_{-0.07}^{+0.08}$	$0.15_{-0.04}^{+0.05}$	$0.08_{-0.02}^{+0.03}$	$0.08_{-0.02}^{+0.02}$	$0.07_{-0.02}^{+0.02}$	$0.06_{-0.02}^{+0.02}$	$0.10_{-0.03}^{+0.03}$	
	Exp. signal	$3.69_{-0.52}^{+0.59}$	$2.14_{-0.33}^{+0.37}$	$1.20_{-0.18}^{+0.21}$	$1.16_{-0.16}^{+0.18}$	$1.17_{-0.16}^{+0.18}$	$1.15_{-0.17}^{+0.19}$	$2.13_{-0.29}^{+0.33}$	
	Observed	2274	65	19	5	3	1	3	
$B^0 \rightarrow \mu^+ \mu^-$ (2012)	Exp. comb. bkg	2491_{-42}^{+42}	$59.5_{-3.2}^{+3.3}$	$13.9_{-1.5}^{+1.6}$	$4.74_{-0.89}^{+1.00}$	$2.10_{-0.61}^{+0.74}$	$0.55_{-0.31}^{+0.50}$	$0.29_{-0.19}^{+0.34}$	
	Exp. peak. bkg	$1.49_{-0.36}^{+0.50}$	$0.86_{-0.22}^{+0.29}$	$0.48_{-0.12}^{+0.16}$	$0.44_{-0.11}^{+0.15}$	$0.42_{-0.10}^{+0.14}$	$0.37_{-0.09}^{+0.13}$	$0.62_{-0.15}^{+0.21}$	
	Exp. cross-feed	$0.63_{-0.09}^{+0.10}$	$0.36_{-0.06}^{+0.07}$	$0.20_{-0.03}^{+0.04}$	$0.20_{-0.03}^{+0.03}$	$0.20_{-0.03}^{+0.03}$	$0.20_{-0.03}^{+0.03}$	$0.36_{-0.05}^{+0.06}$	
	Exp. signal	$0.44_{-0.06}^{+0.06}$	$0.26_{-0.04}^{+0.04}$	$0.14_{-0.02}^{+0.02}$	$0.14_{-0.02}^{+0.02}$	$0.14_{-0.02}^{+0.02}$	$0.14_{-0.02}^{+0.02}$	$0.26_{-0.03}^{+0.04}$	
Observed	2433	59	19	3	2	2	2		

at 90% CL (95% CL), where the lower and upper limit are the branching fractions evaluated at $CL_{s+b} = 0.95$ ($CL_{s+b} = 0.975$) and $CL_{s+b} = 0.05$ ($CL_{s+b} = 0.025$), respectively. These results are in good agreement with the lower and upper limits derived from integrating the profile likelihood obtained from the unbinned fit.

In summary, a search for the rare decays $B_s^0 \rightarrow \mu^+ \mu^-$ and $B^0 \rightarrow \mu^+ \mu^-$ is performed using 1.0 fb^{-1} and 1.1 fb^{-1} of pp collision data collected at $\sqrt{s} = 7 \text{ TeV}$ and $\sqrt{s} = 8 \text{ TeV}$, respectively. The data in the B^0 search window are consistent with the background expectation and the world's best upper limit of $\mathcal{B}(B^0 \rightarrow \mu^+ \mu^-) < 9.4 \times 10^{-10}$ at 95% CL is obtained. The data in the B_s^0 search window show an excess of events with respect to the background-only prediction with a statistical significance of 3.5σ . A fit to the data leads to $\mathcal{B}(B_s^0 \rightarrow \mu^+ \mu^-) = (3.2_{-1.2}^{+1.5}) \times 10^{-9}$ which is in agreement with the SM prediction. This is the first evidence for the decay $B_s^0 \rightarrow \mu^+ \mu^-$.

ACKNOWLEDGEMENTS

We express our gratitude to our colleagues in the CERN accelerator departments for the excellent performance of the LHC. We thank the technical and administrative staff at the LHCb institutes. We acknowledge support from CERN and from the national agencies: CAPES, CNPq, FAPERJ and FINEP (Brazil); NSFC (China); CNRS/IN2P3 and Region Auvergne (France); BMBF, DFG, HGF and MPG (Germany); SFI (Ireland); INFN (Italy); FOM and NWO (The Netherlands); SCSR (Poland); ANCS/IFA (Romania); MinES, Rosatom, RFBR and NRC ‘‘Kurchatov Institute’’ (Russia); MinECo, XuntaGal and GENCAT (Spain); SNSF and SER (Switzerland); NAS Ukraine (Ukraine); STFC (United Kingdom); NSF (USA). We also acknowledge the support received from the ERC under FP7. The Tier1 computing centres are supported by IN2P3 (France), KIT and BMBF (Germany), INFN (Italy), NWO and SURF (The Netherlands), PIC (Spain), GridPP (United Kingdom). We are thankful for the computing resources

put at our disposal by Yandex LLC (Russia), as well as to the communities behind the multiple open source software packages that we depend on.

-
- [1] A. J. Buras, J. Girrbach, D. Guadagnoli, and G. Isidori, *On the standard model prediction for $\mathcal{B}(B_{s,d} \rightarrow \mu^+\mu^-)$* , Eur. Phys. J. **C72** (2012) 2172, [arXiv:1208.0934](#).
- [2] LHCb collaboration, R. Aaij *et al.*, *Tagged time-dependent angular analysis of $B_s \rightarrow J/\psi\phi$ decays at LHCb*, LHCb-CONF-2012-002.
- [3] K. de Bruyn *et al.*, *A new window for new physics in $B_s^0 \rightarrow \mu^+\mu^-$* , Phys. Rev. Lett. **109** (2012) 041801, [arXiv:1204.1737](#).
- [4] DO collaboration, V. M. Abazov *et al.*, *Search for the rare decay $B_s^0 \rightarrow \mu^+\mu^-$* , Phys. Lett. **B693** (2010) 539, [arXiv:1006.3469](#).
- [5] CDF collaboration, T. Aaltonen *et al.*, *Search for $B_s^0 \rightarrow \mu^+\mu^-$ and $B^0 \rightarrow \mu^+\mu^-$ decays with CDF II*, Phys. Rev. Lett. **107** (2011) 191801, [arXiv:1107.2304](#).
- [6] CMS collaboration, S. Chatrchyan *et al.*, *Search for $B_s^0 \rightarrow \mu^+\mu^-$ and $B^0 \rightarrow \mu^+\mu^-$ decays in pp collisions at 7 TeV*, JHEP **04** (2012) 033, [arXiv:1203.3976](#).
- [7] ATLAS collaboration, G. Aad *et al.*, *Search for the decay $B_s^0 \rightarrow \mu^+\mu^-$ with the ATLAS detector*, Phys. Lett. **B713** (2012) 387, [arXiv:1204.0735](#).
- [8] LHCb collaboration, R. Aaij *et al.*, *Strong constraints on the rare decays $B_s^0 \rightarrow \mu^+\mu^-$ and $B^0 \rightarrow \mu^+\mu^-$* , Phys. Rev. Lett. **108** (2012) 231801, [arXiv:1203.4493](#).
- [9] LHCb collaboration, A. A. Alves Jr. *et al.*, *The LHCb detector at the LHC*, JINST **3** (2008) S08005.
- [10] T. Sjöstrand, S. Mrenna, and P. Skands, *PYTHIA 6.4 physics and manual*, JHEP **05** (2006) 026, [arXiv:hep-ph/0603175](#).
- [11] D. J. Lange, *The EvtGen particle decay simulation package*, Nucl. Instrum. Meth. **A462** (2001) 152.
- [12] GEANT4 collaboration, J. Allison *et al.*, *Geant4 developments and applications*, IEEE Trans. Nucl. Sci. **53** (2006) 270.
- [13] GEANT4 collaboration, S. Agostinelli *et al.*, *GEANT4: a simulation toolkit*, Nucl. Instrum. Meth. **A506** (2003) 250.
- [14] P. Golonka and Z. Was, *PHOTOS Monte Carlo: a precision tool for QED corrections in Z and W decays*, Eur. Phys. J. **C45** (2006) 97, [arXiv:hep-ph/0506026](#).
- [15] I. Belyaev *et al.*, *Handling of the generation of primary events in GAUSS, the LHCb simulation framework*, Nuclear Science Symposium Conference Record (NSS/MIC) **IEEE** (2010) 1155.
- [16] M. Clemencic *et al.*, *The LHCb simulation application, GAUSS: design, evolution and experience*, J. of Phys.: Conf. Ser. **331** (2011) 032023.
- [17] R. Aaij and J. Albrecht, *Muon triggers in the High Level Trigger of LHCb*, LHCb-PUB-2011-017.
- [18] V. V. Gligorov, C. Thomas, and M. Williams, *The HLT inclusive B triggers*, LHCb-PUB-2011-016.
- [19] G. Lanfranchi *et al.*, *The muon identification procedure of the LHCb experiment for the first data*, LHCb-2009-013.
- [20] Particle Data Group, J. Beringer *et al.*, *Review of particle physics*, Phys. Rev. **D86** (2012) 010001.
- [21] L. Breiman, J. H. Friedman, R. A. Olshen, and C. J. Stone, *Classification and regression trees*, Wadsworth international group, Belmont, California, USA, 1984.
- [22] R. E. Schapire and Y. Freund, *A decision-theoretic generalization of on-line learning and an application to boosting*, Jour. Comp. and Syst. Sc. **55** (1997) 119.
- [23] CDF collaboration, A. Abulencia *et al.*, *Search for $B_s^0 \rightarrow \mu^+\mu^-$ and $B_d^0 \rightarrow \mu^+\mu^-$ decays in $p\bar{p}$ collisions with CDF II*, Phys. Rev. Lett. **95** (2005) 221805, [arXiv:hep-ex/0508036](#).
- [24] T. Skwarnicki, *A study of the radiative cascade transitions between the Upsilon-prime and Upsilon resonances*, PhD thesis, Institute of Nuclear Physics, Krakow, 1986, DESY-F31-86-02.
- [25] LHCb collaboration, R. Aaij *et al.*, *Measurement of the ratio of fragmentation fractions f_s/f_d and dependence on B meson kinematics*, LHCb-PAPER-2012-037, in preparation.
- [26] J. H. Morata *et al.*, *Measurement of trigger efficiencies and biases*, LHCb-2008-073.
- [27] A. Datta, *Semi-leptonic decays of Λ_c and Λ_b baryons involving heavy to light transitions and the determination of $|V_{ub}|$* , [arXiv:hep-ph/9504429](#).
- [28] W. Wang and Z. Xiao, *Semi-leptonic decays of $B/B_s \rightarrow (\pi, K)(l^+l^-, lv, \bar{\nu}\nu)$ in the perturbative QCD approach beyond the leading-order*, [arXiv:1207.0265](#).
- [29] LHCb collaboration, R. Aaij *et al.*, *Measurement of b hadron production fractions in 7 TeV pp collisions*, Phys. Rev. **D85** (2012) 032008, [arXiv:1111.2357](#).
- [30] CDF collaboration, F. Abe *et al.*, *Observation of the B_c meson in $p\bar{p}$ collisions at $\sqrt{s} = 1.8$ TeV*, Phys. Rev. Lett. **81** (1998) 2432, [arXiv:hep-ex/9805034](#).
- [31] D. Melikhov and N. Nikitin, *Rare radiative leptonic decays $B_{d,s} \rightarrow l^+l^-\gamma$* , Phys. Rev. **D70** (2004) 114028.
- [32] LHCb collaboration, R. Aaij *et al.*, *First observation of the decay $B^+ \rightarrow \pi^+\mu^+\mu^-$* , [arXiv:1210.2645](#).
- [33] A. L. Read, *Presentation of search results: the CL_s technique*, J. Phys. **G28** (2002) 2693.